Journal of Electrical and Electronics Engineering (IOSR-JEEE)
e-ISSN: 2278-1676, p-ISSN: 2320-3331, Volume 20, Issue 6 Ser. 1 (Nov. – Dec. 2025), PP 31-36
www.iosrjournals.org

Electron Microscopic And X-Ray Line Observations On Microstructures Of Synthesized ZnS: Mn^{+2} Nanocrystalline Thin Films

K Zeetibala, M Rajesh Singh, M Malemnganbi And K Kunjabali Singh
Department Of Physical Science
Khongnangthaba University, Khurai-795010, Manipur, India

Abstract:
ZnS: Mn^{+2}-ions thin films in the range 2at.%≤ x≥10 at.% concentrations thin films were synthesized on Silicon wafer substrates by SILAR (Successive Ionic Layer Adsorption and Reaction) technique. The surface morphology, micro structures, micro-stress and strains and dislocation density in the films were critically studied using FESEM and XRD techniques. The X-rays line spectral profiling showed maximum reflection peak intensity along (110) at 2at.%, (421) plane at 4at.%, (100) planes at 6at.% and 8at.% Mn^{+2}-ions. The as deposited ZnS:Mn^{+2} films showed Cubic zinc sulphide structures with different reflection planes preferably f.c.c. cubic at 8at.%Mn^{+2}-ions concentration. The observed lattice parameters in the host ZnS doped films in the wide range of X-rays reflection intensity were found decreasing with increasing of the intensity and closed to the standard values at 2at.% (521), 4at.% (421), 6at.% (300) and 8at.% (311) planes. The evaluated ZnS particle sizes were found in the nano-size regime with increase of Mn^{+2}-ion concentrations. The films showed enhanced of dislocation density but to decrease in microstrains with increase of doping concentration. The as deposited doped ZnS nanocrystalline films showed comparatively higher micro-stress at 100% X-rays peak intensity from the average values at all levels of peak intensity.

Keywords:*Zinc sulphide thin films, SILAR, FESEM, XRD, microstructures*

Date of Submission: 08-11-2025 Date of Acceptance: 18-11-2025

I. Introduction:

Bulk Zinc Sulphide (ZnS) with a wide direct band gap of 3.7eV in near UV-region, is one of the prominent members of II-VI inorganic compound semiconductors. The bulk crystalline form of ZnS exits in two different forms –(i) Spharalite (Cubic) and (ii) Wurtzite (Hexagonal). ZnS is naturally white in colour. However, its colour may change to yellowish or grayish depending on impurities present or crystalline nature. ZnS is insoluble in water but dissolves in acids. Besides, materials at nanoscale show significantly noble properties entirely different from their bulk counterparts due to high surface area to volume ratio on account of quantum confinement effect [1,2]. At this effect, materials consist of a large number of very small potential wells in which excitons are trapped and electronic energy levels become discrete [3,4]. Therefore, a large number scientists and researchers all over world from all branches of material science, chemical science, biological science, medical science are engaged actively in nanoscience and nanotechnology researches by synthesizing materials at nanoscale of 1nm -100nm in atomic diameter (1nm=10^{-9}m) using different techniques. Depending on the nature of the choice materials, time and economical points of view, materials can be synthesized bydifferent techniques*viz* Chemical Bath Deposition (CBD), Electrode Deposition (ED), RF Sputtering, Thermal Evaporation (TE), Successive Ionic Layer Adsorption and Reaction (SILAR), Hydrothermal process, Spin Coating etc. In this paper, we are using SILAR method for synthesis work and presenting surface topology and other microstructures associated with other parameters in the films. Because, the structural parameters of thin films play important parts correlating to find fabrication of new technological devices and applications. As for the host sample films, the energy band gap of ZnS closed to in near UV regionand makes it suitable for fabrication of blue light emitting diodes (BLEDs) [5] and other opto-electronic devices, electroluminescence [6], cathodoluminescent displays, multilayer dielectric filters [7,8]. A large number of people have given considerable efforts towards the synthesis of ZnS nanocrystals using different techniques such as thermal evaporation, spray pyrolysis molecular beam epitaxy, etc. Most of the researchers have used equal concentration of Zn^{2+} and S^{-}ion precursors in the synthesis works [9]. However, reports on variation of Zn^{2+} and S^{-} ion concentrations in synthesis of ZnS nanocrystals by different chemical methods show unsubstantial works.

II. Materials And Method:

In the synthesis work, we used high purity Zinc Acetate, $Zn(CH_3COO)_2$ (AR Grade) for Zn^{+2}-ion source, (ii) Thiourea, $CS(NH_2)_2$ (AR Grade) for S^{-2} –ions source, (iii) ManganiseChloride , $MnCl_2$for doping agent (iv) Ammonia solution (v) PVA (vi) Trisodium Citrate as reducing agent. The synthesis work using SILAR technique required the following steps:

*Step-(a).*We dissolved 4.39gms (*estimated by calculation*) of Zinc Acetate (ZA), *$Zn(CH_3COO)_2$*in 50ml of DI water and stirred for 30mins.

*Step-(b).*We dissolved 2gms of PVA (Polyvinyl Alcohol) in 100ml DI water and stirred at 70^0C for 30mins till PVA dissolves.

Step-(c). Then 50ml of ZA was mixed with 50ml PVA solution in 250ml beaker

Step-(d). Now we prepared 0.2M solution of $MnCl_2$ by dissolving 0.184gm of it in 5ml DI water, stirred for 5mins and added to the above mixture.

The precursor of step (d) was mixed with 10ml TSC solution and a few drops of ammonia solution was dropped to adjust the pH of solution at 10 with constant stirring.

Properly cleaned Silicon Wafer substrates (4nos.) were clamped vertically in the solution for 24hrs to adhere the Zn^{+2}-ions to the substrates.

Lastly, we prepared 0.2M solution of thiourea, $CS(NH_2)_2$ by dissolving 1.52gm of it in 50ml. DI water, to which 10ml of TSC solution was added. Further, a few drops of ammonia solution were added to adjust the pH value at ≈ 10 with constant stirring for 5mins. The Zn^{-2} ions pre-deposited substrates were dipped vertically into it for 24hrs whence Zn^{+2} –ions reacted with S^{-2}-ions to produce ZnS thin films on to the substrates.

III. Results And Discussion

3.(a) Effect of doping concentration on structural properties:

Fig.1. (a,b,c & d) show the XRD patterns of the grown ZnS:Mn^{+2} phosphor at 2at.%, 4at.%, 6at.% and 8at.% at 300^0C annealed temperaturesubstrate The spectral analysis of the sample films clearly reveals the crystalline thin films.The diffraction patterns clearly reveal maximum

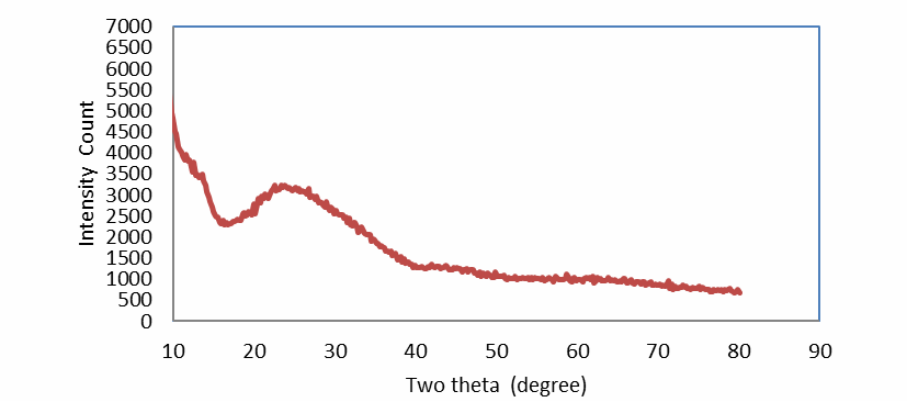

(100)

(421)

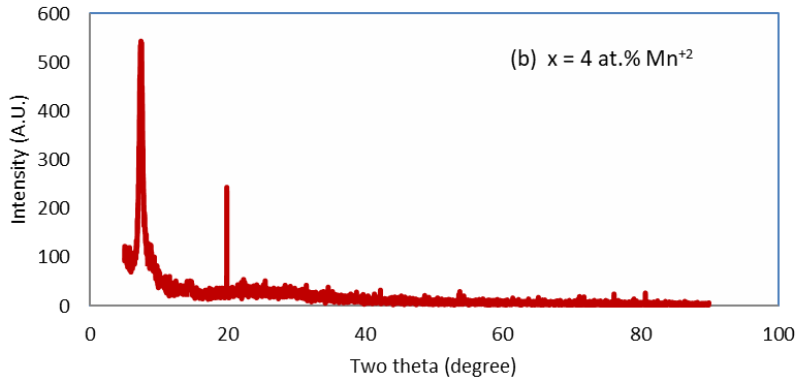

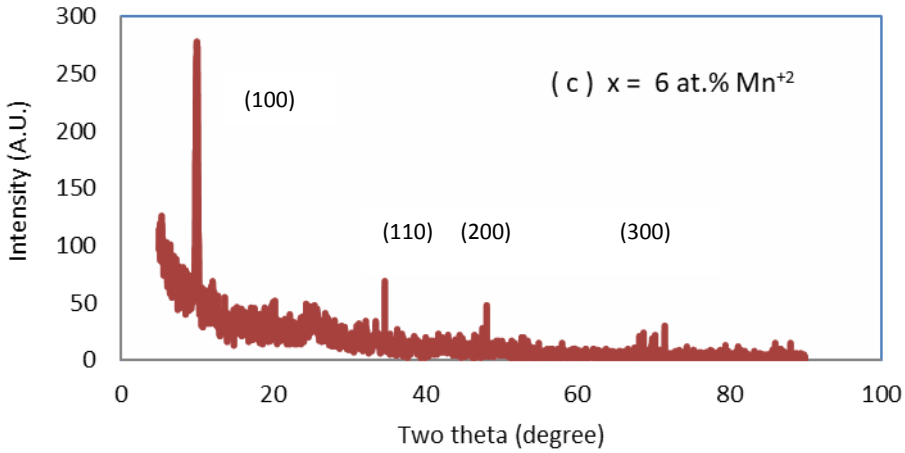

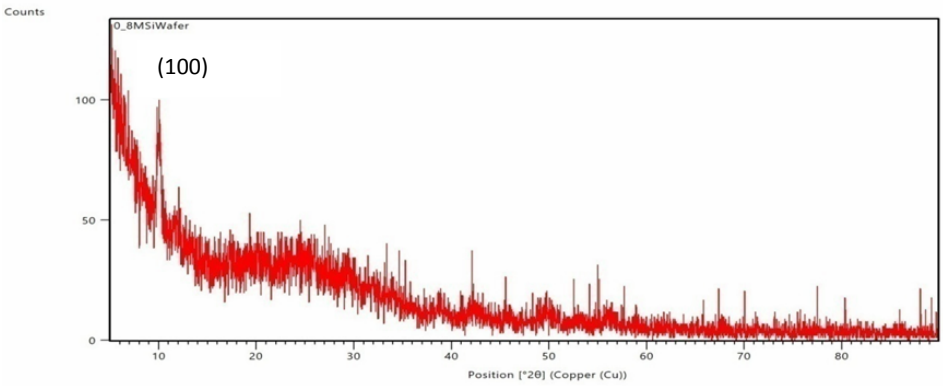

Fig. 1(a,b,c & d) ZnS: Mn^{+2}– ions at different doses XRD pattern thin films.

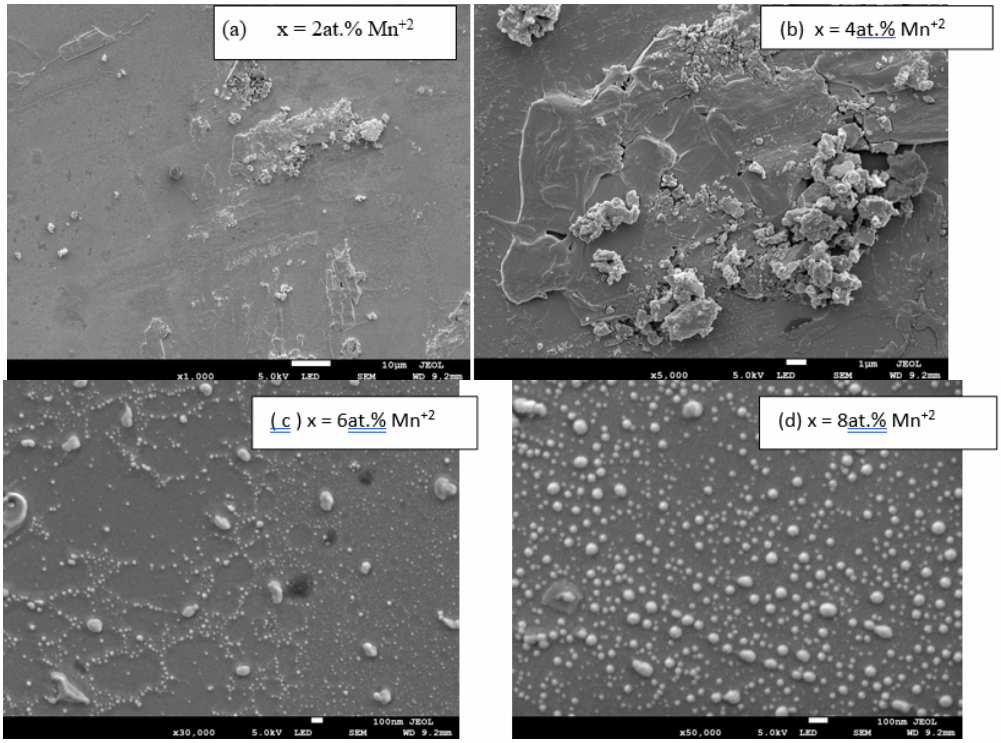

Fig. 2. (a, b, c & d) FESEMsurface images of ZnS : Mn $^{+2}$ –ions thin films at different doses.

Table-1. Observed lattice parameters in synthesized ZnS : Mn^{+2} –ions

Mn^{+2} dose	Rel. X-rays int.	2Θ-value (degree)	(hkl)	JCPDS *a*-value (Å)	$a_{cal.}$ (Å)	JCPDS d-value (Å)	d_{cal} (Å)
2 at.%	5420	5.15		5.410		1.90	
	26.92	13.31	100		8.642		6.642
	39.28	18.42	100		4.812		4.812
	13.89	19.14	100		4.631		4.631
	100.00	22.08	110		5.686		4.021
	80.58	59.09	220		4.416		1.562
	53.34	64.53	321		5.397		1.442
	9.06	65.80	321		5.304		1.418
	49.39	66.06	321		5.286		1.412
	36.00	70.41	400		5.343		1.336
	9.87	73.33	421		5.471		1.290
	45.91	80.99	421		5.434		1.186
4 at.%	100.00	7.45					
	3.29	14.68	100		6.028		0.028
	5.16	80.75	421		5.447		1.189
6 at.%	100.00	10.11	100		8.742		8.742
	11.47	12.12	100		7.294		7.294
	6.61	19.03	100		4.657		4.657
	10.90	20.05	110		6.256		4.424
	2.96	31.69	200		5.640		2.827
	3.60	38.64	120		5.204		2.327
	3.02	50.00	300		5.466		1.822
8 at.%	100.00	10.03	100		8.801		8.801
	12.19	38.80	210		5.184		2.318
	15.42	42.38	112		5.217		2.129
	17.65	55.93	311		5.446		1.642
	4.28	89.21	422		5.372		1.096

reflection peaks along (110) plane at 2at.%,, 6at.% and 8at.% of Mn^{+2}-ions concentrations while no reflection plane can be defined at 4at.% as $2\Theta \leq 10^0$.The FESEM surface morphology of the synthesized ZnS: MN^{+2} thin films (Fig. 1) show that the agglomeration and particle sized of the ZnS films decrease nonlinearly with increase of the implanted Mn^{+2}- ions in the films.The multiple peaks intensity in the XRD spectra show that the as deposited Mn+2-ions ZnS films are found to be non amorphous polycrystalline , the nature of which will be

defined by grain sizes in the films. The (hkl) X-rays diffraction planes corresponding to peak intensity were calculated from the Bragg's relation

$$2dSin\Theta = n\lambda \quad (1)$$

Whence $Sin^2\Theta = (\lambda^2/4a^2)N$, (2)
where $h^2 + k^2 + l^2 = N$, $n = 1$ (1^{st} order diffraction)and $\lambda = 1.54$Å.

The lattice parameters ***a and d*** – values of were calculated from the relations

$$a = (\lambda/2Sin\Theta) \times \sqrt{(h^2 + k^2 + l^2)} \quad (3)$$

$$d = \lambda\text{-}2Sin\Theta \quad (4)$$

The grain or particle sizes were calculated from the Scherr relation [10] at 100% intensity of the X-rays

$$D = k\lambda/\beta Cos\Theta \quad (5)$$

where the value of shape factor k is taken as 0.94, β, the width the peak at half of maximum peak intensity (FWHM) expressed inradian and θ the Bragg angle and were found between 21.16nm to 100.41nm as shown in Table-2. The evaluated *a* and *d* values are shown in Table -1.The crystal structures of the synthesized host sample films were determined from the relation [11]

$$Sin^2\Theta_1/Sin^2\Theta_2 = (h_1^2 + k_1^2 + l_1^2)/(h_2^2 + k_2^2 + l_2^2) \quad (6)$$

and were found to be cubic as shown in Table-2.

Table-2. Crystal structure of ZnS films at Mn^{+2}- ions doping concentrations

Sample ZnS :Mn^{+2}	$h_1k_1l_1$	$h_2k_2l_2$	Θ_1 (degree)	Θ_2 (degree)	$Sin^2\Theta_1/Sin^2\Theta_2$	$(h_1^2+k_1^2+l_1^2)/(h_2^2 + k_2^2 + l_2^2)$	Cry. Str.
2at.%	100	110	9.572	11.039	0.75	0.5	fcc
4at.%	100	421	7.338	40.373	0.04	0.07	
,6 at.%	100	110	8.516	10.023	0.72	0.5	fcc
8at.%	210	112	19.388	21.194	0.84	0.83	fcc

(b) Dislocation density, micro-stress and strains:

The as deposited ZnS : Mn^{+2} nanocrystalline thin films grown under suitable experimental conditions were observed under various micro-stress and strains on account of some physical factors like variations of lattice parameters and oxygen vacancies. The micro-strains were calculated using the relation [12,13]

$$\varepsilon = \beta_{2\theta} [Cot\theta/4] \quad (6)$$

The stresses caused by some thermal expansion co-efficient of the films and haphazard grain size orientations were calculated using the relation [14,15]

$$S = E/2\gamma(a_0 - a)/a_0 \quad (7)$$

where $a_0$and *a* are lattice parameters of ZnS bulk and thin film materials, γ the Poisson ratio taken as 0.32 and E the Young's Elastic Moduli as 74.5[13]. The lattice micro stress and strains were calculated separately (i) at 100% X-rays intensity and (ii) the average of a_{cal}-values of the films corresponding to sets of Mn^{+2}-ion doping. The dislocation density in the films on account of oxygen vacancies attributed lattice strains and were calculated using Willamson and Smallman's relation [16-18]

$$\delta = 1/D_{hkl}^2 \quad (8)$$

where D_{hkl} is the grain or particle size. The values of grain sizes, dislocation density, microstress and strains are shown in Table-3.

Table-3.Observed grain sizes, dislocation density, micro-stress and strains at 100% intensity

Sample ZnS :Mn^{+2}	FWHM (2Θ) (degree)	Grain size (nm)	Dislocation density (δ) (lines/m^2)	Micro-stress (GPa)	a_{cal}-value (Å)	JCPDS *a*-value (Å)	Micro-strains (ε)
2at.%	0.059	100.41	$9.92x\ 10^{13}$	5.95	5.686	5.410	$50.03x10^{-2}$
4at.%	0.433	19.18	$27.18x10^{14}$				$50.01x10^{-2}$
,6 at.%	0.138	60.27	$2.75x10^{14}$	72.17	8.742		$20.00x10^{-1}$
8at.%	0.394	21.16	$22.33x10^{14}$	72.97	8.801		$20.00x10^{-1}$

Table-4. Average micro-stress below 100% intensity

Sample ZnS :Mn^{+2}	Relative Intensity	a_{cal}-value (Å)	Aver. value of a_{cal}-value (Å)	JCPDS *a*-value (Å)	Micro-stress (GPa)
2at.%	26.92	8.642	5.493	5.410	1.79
	39.28	4.812			
	13.89	4.631			
	80.00	4.416			
	53.00	5.397			
	9.06	5.304			
	49.39	5.286			
	6.12				
	36.00	5.343			
	9.81	5.471			
	45.90	5.434			
4at.%	3.28	6.028	5.738		7.05
	5.16	5.447			
6at.%	11.47	7.294	5.768		7.68
	6.61	4.657			
	10.90	6.256			
	10.21	4.942			
8at.%	12.19	5.184	6.004		12.78
	15.42	5.217			
	1`7.65	5.446			
	4.78	5.572			

It is observed that the grain sizes in the films are found between 19nm to 100nm in the nano-scale with negligible micro-strains but stressedconsiderably between nano-particles. These nano-stresses areobserved increasing linearly with increase of Mn^{+2}-ions concentration in the doped ZnS thin films. However, the average value of nano-stress in the synthesized doped ZnS thin films are observed less than the corresponding values at 100% X-rays peak intensity. Lower stress on nanoparticles in thin films will have significant contributions in the fabrication of nano-technological device and applications.

IV. Conclusion

The as grown ZnS :Mn^{+2} –ions films show fcc Cubic zinc sulphide structure with different reflection Planes. The observed lattice parameters *a* and*d* –values are found decreasing with increasing of the intensity of X-rays and closed to the standard values at 2at.% (521), 4at.% (421), 6at.% (300) and 8at.% (311). The evaluatedZnS doped grain sizes are found between 20nm to 100nm in the nanometer range anddecrease relatively with increase of doping ions. The thin films are found highly stressed between lattice nanoparticles at 100% relative intensity which is relatively enhanced with increase of doping ions. It is also observed that the films show lowernanoo –stress below 100% peak intensity at all levels of peak intensity which will find significant contribution to fabrication of nano based device and applications.

Acknowledements

The authors are thankful to SAIF, Guwahati University for providing XRD facilities and CIF, Tezpur University, Assam for FESEM and also some XRD facilities in this research works.

References

[1]. Emil Roduner, Nanomaterials Size Dependent Phenomena, R S C Publishing, Royal SocietyOfChemistry, 2006 Chap. 1, Page 2.
[2]. G Mohan Kumar, Nanotechnology Nanomaterials AndNanodevices, Narora PublishingHouse Pvt. Ltd (2016) 1.12.
[3]. Schmid Et AI, Nanotechnology Assessment AndPerspectives, Mackmillan India Ltd. (2006)79
[4]. M Dinendra Singh AndKKunjabali Singh, IOSR Journal OfApplied Physics (IOSR-JAP) Vol. 15, Issue 5 Ser. 1 (Sept-October, 2023) 69-72
[5]. Pawan Kumar, Arvind Kumar, P N Dixit AndT P Sharma, Indian Jr. Of Appl. Phys. Vol. 44 (2006)690
[6]. Jyoti Borah, J Barman, KC Sarma, Chalcogenide Letters, Vol. 5, 9, Sept (2008) 201
[7]. Li Dyuer A M, Appl. Optics, 18 (1979)2979
[8]. Jones P L, Moore D M And Smith D C, Journal Physics E(1976) 312
[9]. Suyver J F, Weister S F, Kelly J JAnd Meejerenk A, Nano Lett. 1(2001)429
[10]. H P Klug AndL E Alexander, X-Ray Diffraction Proceedures, New York, John Willey &Sons Inc., (1954) 490
[11]. Navaneet Gupta, R C Gupta, Principles OfMaterials Science AndEngineering, Dhanapat Rai &Co. Pvt. Ltd. (2001) 79
[12]. Suchetra Sen, S K Halder AndS P Sengupta, J. Phys. Soc., Jpn, 38 (1975) 1644
[13]. K Kunjabali Singh AndH L Das, Indian J. Phys., 82 (6) (2008)185-693
[14]. C K Dey, N K Misra AndT B Gosh, Indian J. Phys, 69A (2) (1995)261
[15]. C K Dey, N K Misra AndT B Gosh, Indian J. Phys, 71A (5) (1997) 530
[16]. Mahaligam T, Thanikarasan S And Chandramohon R, Mater. Sci Eng B, 174(2010)236
[17]. M Rasmani Devi AndK Kunjabali Singh, International Journal OfEngineering AndTechnical Research (JETR) Vol. 9, Issue 12, Dec., (2019) 1-4
[18]. K Manikandan, P Mani, Fermi Hilbert Janbaraj, T Dominie Joshef, V Thangaraj, C Samendra Dilip AndJ Josheph Price, Indian Journal OfPure &Applied Physics, Vol. 52, May 2014 354-359